

ARTICLE

# Allowed Spatial Transitions and Cancellation of the Richardson-Langmuir Ban

Ordin S.V.\*

Ioffe Institute RAS., Russia

---

ARTICLE INFO

*Article history*

Received: 18 June 2021

Accepted: 23 June 2021

Published Online: 25 June 2021

---

*Keywords:*

Potential barrier

Ballistic model

Spatial transition of electrons

Electron condensation

Local Thermo-EMF

p-n junctions

---

ABSTRACT

The ancient emission formulas of Langmuir and Richardson entered the calculations of subtle effects in semiconductor devices as basic ones. But, in the physics of semiconductor devices, these models have long played a purely decorative role, since they can describe in the most rough approximation only individual sections of the  $I - V$  characteristic. But it is precisely the fact that these formulas are basic when describing the barrier current-voltage characteristics (CVC) and prevented the consideration and use of thermoelectric effects in materials on a nano-scale. Thus, as these basic emission models actually imposed a ban on the MEASURABILITY of local thermoelectric effects, the existence of which has already been proven both phenomenologically and experimentally.

The quantum transition technique is based on classical models. But it can also be used to correct these classic formulas. The calculation of the spatial transition of electrons over the potential barrier, taking into account the polarity of the kinetic energy, gives currents that are significantly higher than the currents of Langmuir and Richardson, including in the initial section of the  $I - V$  characteristic. Moreover, ballistic currents are concentrated at energy levels close to the threshold. This effect of condensation of electrons flowing down the barrier transforms the "anomalous" Seebeck coefficients into normal MEASURABLE Local Thermal EMF, including in p-n junctions.

## 1. Introduction

Someone not stupid said: "Science begins where Mathematics begins." But at the time of Newton, in fact, there was still no separation of Physics and Mathematics. And Isaac Newton, in parallel with Gottfried Leibniz, resolving Zeno's aporia about Achilles and the tortoise, laid the foundations of a new branch of Mathematics - Differential Calculus. But Physics was built not only with the help of new sections of Mathematics. Many Physical Laws were substantiated in the simplest case with the

help of algebraic equations. And the contradictions that had accumulated in uncombed Physics at the end of the last century were taken up not by a recognized scientist, but by the senior telegraph operator Heaviside, who, it would seem, in solving a particular electrodynamic problem first began to use complex numbers, and then tensors. The latest mathematics, already developed (by the same Riemann), brought by Heaviside into Physics, in fact, brought Maxwell's electrodynamics to a modern form, implicitly gave Schrödinger an operator approach, prompted Einstein to build the Theory of Relativity within

---

\*Corresponding Author:

Ordin S.V.

Ioffe Institute RAS., Russia

Email: [stas\\_ordin@mail.ru](mailto:stas_ordin@mail.ru)

the framework of Geometry extended by Riemann.

Thus, by introducing independently advanced Mathematics into primitive Physics, Heaviside actually raised entire sections of modern Theoretical Physics to a pedestal. And this, in principle, would be nice if the entire Physics described by dense formulas began to be brought up to the mathematical level of these sections. But the editors artificially torn these sections away from all of Physics. And, referring only these (Theoretical) sections to Fundamental Physics, they did more harm than they helped. And, thus, they hurt themselves, as they broke away from reality. That is why, in fact, both the Quantum Theory and the Theory of Relativity went to the wrong steppe. And to restore the connection of THEM with reality, it was necessary to rethink and rewrite a wider layer of Physics at the modern mathematical level. And because it is directly linked to these theoretical sections in ELEMENTARY MODELS. And because this is how it was possible to understand why “to the wrong steppe” - the developers in “smart” mathematical calculations actually drowned the Ideas of Planck-Einstein, and, at the same time, and Mat. Heaviside physics.

So the completion of the article “Fundamentals of Quantization” required compliance with Einstein’s NECESSARY condition: “Some equations of classical mechanics can be rewritten in operator form”, i.e. rigor was also required in the classical equations used for rewriting [1].

The completion of this work required a rethinking of what was actually put by Planck in the Basics of Quantization, the fascination with the waves of HIS matter - the Heaviside’s impedance (himself) pushed also far? As well as his Electromagnetic Theory of Gravity [2].

This required a strict account of both in Classical Mechanics and in the Heaviside Impedance of the Irreversibility of Time [3].

And the latter is already directly related to Thermodynamics, which since the time of Boltzmann has so far remained uncombed, since it uses a traditional frame, not an orthogonal one.

But combing both the Fundamentals of Thermostatistics (which was mistakenly called Thermodynamics) and the Fundamentals of Thermodynamics proper, the Linear Approximation of which was called Nonequilibrium Thermodynamics, is a big independent work. So far, I have limited myself only to the refinement in the description of Thermoelectric Processes on the basis of the traditional thermodynamic reference [4,5].

And this phenomenological examination was enough to understand:

(1) The traditional Onsager-Ioffe Theory of Thermoelectricity describes only diffuse processes, which

Ioffe used for heavily doped semiconductors.

And this alone turned out to be enough to show that modern thermoelectric technology has reached the diffuse limit of the efficiency of the thermoelectric devices being developed [6].

(2) And the lightly doped semiconductors, which dropped out of consideration, are barrier structures that make it possible to dramatically increase the efficiency.

But the high-voltage thermoelectric power discovered back in the fifties of the last century by Tauts in its first transistors, since they did not fit into the phenomenology of thermoelectricity, were classified as “anomalous”, and the estimates by Richardson’s formula of currents above the potential barrier gave such small values that they were practically referred to UNMEASURABLE.

## 2. Experimental, Results and Discussion

### 2.1 Semiconductor Barriers

Initially, research was carried out on the contacts of various semiconductors. But later, most of the results discussed in this article were obtained on structures grown on silicon substrates and on aluminum nitride substrates.

And experiments have shown that the local thermopower of a micron p-n junction prevails over the diffuse thermopower of a 300 micron silicon substrate.

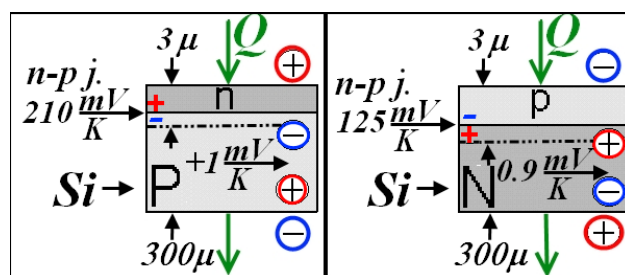


**Figure 1.** The thermopower of a silicon structure with a micron layer of inverse conductivity measured by the direct contact method gives a total voltage determined by the polarity of the n-n junction and exceeding the thermopower of a silicon substrate (silicon wafer) without an inverse layer by an order of magnitude.

The inertness of academic science, which did not recognize the “immeasurable” effects, which already significantly surpassed analogues based not only on diffuse thermoelectric effects, but also on the basis of the photoelectric effect, naturally slowed down the introduction of devices based on Local Thermo-EMF [7-10].

But, as they say, everything in the world is interconnected. The Quantum Theory of Solids, despite the errors in the Basics of Quantization, methodically in calculations has advanced much further than the dense

formulas of Richardson and Langmuir. But their analysis within the framework of the Quantum Solid State Theory helped to advance in the very understanding of the Basics of Quantization - Spatial Quantum Transitions.

The laws of conservation of energy and momentum rule both the classical and the quantum world. In quantum calculations, they are methodically used in the space of (quasi) momenta. Those zone patterns are constructed for ALLOWED states and transitions between them, in fact, in the velocity space. And strictly speaking, only transitions to UNRESOLVED states are forbidden, which give a low probability and UNMEASURABLE currents. So the real MEASURABLE currents above the potential barrier (which in practice have long been used in electronics, but not in thermoelectricity), it was just necessary to honestly count the transitions between the ALLOWED states on the emitter and collector. But for such calculations, it is necessary to take into account the polarity of the kinetic energy of electrons relative to the electric field in the region of the potential barrier.

### 2.2 Vacuum Barrier (Brief Historical Background)

The giant differences in currents through semiconductor potential barriers from those predicted by theory and, all the more, the high detectivity of detectors based on thermoelectric barrier effects prompted a thorough experimental analysis of the properties of the vacuum barrier, which served as the basis for calculating semiconductor barriers.

Initially, the Langmuir and Richardson formulas were constructed for thermionic emission<sup>[11]</sup>:

$$J = \frac{\sqrt{2}}{9\pi} \sqrt{\frac{e}{m}} \cdot \frac{1}{d^2} \cdot U^{3/2}, \quad J_e = (1-r) AT_h^{1/2} \exp\left(-\frac{e\phi_h}{kT_h}\right) \quad (1)$$

Where in the Langmuir formula  $d$  false is the barrier thickness, and  $U$  false is the potential difference across it and where  $A$  false - the Richardson constant,  $\phi_h$  false and  $T$  false - the work function and temperature (of the cathode, in thermal emission), respectively, and  $r$  false - the average value of the reflection coefficient of electrons at the boundary, which is small and, in the analysis, we will further assume that the first bracket is equal to 1.

These well-known formulas for the electron flux, both Langmuir and Richardson, were grossly grounded at the microscopic level as well<sup>[12]</sup>. Langmuir's formula - under the assumption of the initial zero velocity of all electrons above the barrier and its increment due to the electric field. And Richardson's formula - when taking into account (in the Brillouin zone) only those electrons whose velocity vector is directed towards the interface. In fact, the Richardson model took into account only the

difference between the electron concentrations at the emitter and collector above the maximum of the potential barrier, which arises when the field is applied, multiplied by the average thermal velocity of the electrons.

$$\int_0^\infty \int_0^\infty \int_0^\infty v_x n_0^* e^{-\left(\frac{m}{2kT}(v_x^2+v_y^2+v_z^2)+\frac{\phi}{kT}\right)} dv_z dv_y dv_x = n_0^* 2\pi \left(\frac{kT}{m}\right)^2 \cdot e^{-\frac{\phi}{kT}} \quad (2)$$

which corresponds to the average thermal velocity along one coordinate  $\bar{v}_x^* = \sqrt{\frac{2}{\pi}} \cdot \sqrt{\frac{kT}{m}}$  (the root mean square is equal to  $\sqrt{\frac{kT}{m}}$ ) multiplied by the electron concentration in half of the Brillouin zone  $n^* = \frac{1}{2} n_0^* \left(2\pi \frac{kT}{m}\right)^{3/2}$ .

For a frequently used one-dimensional view, Formula 2 is simplified:

$$\int_0^\infty (v_x) n_0^* e^{-\left(\frac{m}{2kT}(v_x^2+v_y^2+v_z^2)+\frac{eU}{kT}\right)} dv_x \Rightarrow J_2 = n_0^* \frac{kT}{m} e^{-eU^*} \quad (3)$$

Due to the roughness of the original Richardson model, the theoretical does not correspond to the experimental, adjustable values, even in order of magnitude. And neither Langmuir nor Richardson's formula (2) even gives a qualitative description of the experimental current-voltage characteristics of barriers in a sufficiently wide range, even for an "ideal" vacuum barrier<sup>[13]</sup> (Figure 2). Therefore, they can be used only when adjusting the I – V characteristic in a narrow voltage range.

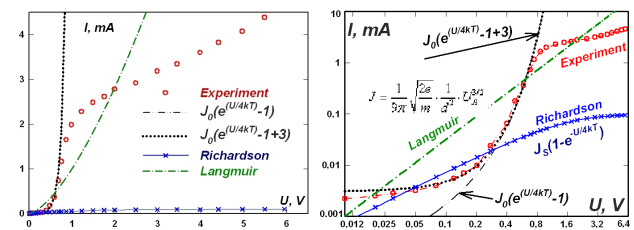


Figure 2. Experimental and Langmuir – Richardson I – V characteristics for a vacuum barrier.

Nevertheless, it was the estimates by the Richardson formula<sup>[13,14]</sup> that imposed a "ban" on the experimentally observed large thermopower, transferring them to the category of anomalies<sup>[15]</sup>.

## 3. Theory

### 3.1 Fragmented Description of Spatial Transitions

To obtain a rough dependence of current on voltage, one



The Richardson model takes into account only electrons with positive initial velocities. So the obtained first addition to the emitter current is not taken into account that when the current passes through the barrier boundary, the momentum and energy shift affects all electrons of the parabolic zone. However, it is obvious that electrons with low negative velocities can also change the sign of the velocity to a positive one. Therefore, we will consider one more addition to the more refined Richardson current from the energy range denoted in Figure 3a as A1. The sum of the partial contributions of these electrons also gives a positive (second and not small) addition to the total current:

$$\Delta J_{2E} = n_0 \frac{kT}{m} \left( 1 + \frac{\pi}{2} e^{-\frac{eU^*}{2}} \left( \text{BesselJ} \left[ 0, \frac{eU^*}{2} \right] + \text{BesselJ} \left[ 1, \frac{eU^*}{2} \right] \right) e^{U^*} - e^{-eU^*} \right) \quad (9)$$

But electrons with large negative starting velocities due to the electric field at the barrier also have a positive addition to the velocity, which leads to a positive (third) addition to the emitter current:

$$\Delta J_{3E} = n_0 \frac{kT}{m} \left( e^{-\frac{eU^*}{2}} - \frac{\sqrt{\pi}}{2} \text{MeijerG} \left[ \left\{ \left\{ \left\{ \frac{3}{2} \right\} \right\}, \left\{ \left\{ 0, 1 \right\}, \left\{ \right\} \right\}, eU^* \right] \right) \quad (10)$$

So the total emitter - the modified Richardson current (formula 5), will include the total addition

$$J_{R1}^* = J_{R1} + \Delta J_{1E} + \Delta J_{2E} + \Delta J_{3E} = J_{R1} + \Delta J_{\Sigma E} \quad (11)$$

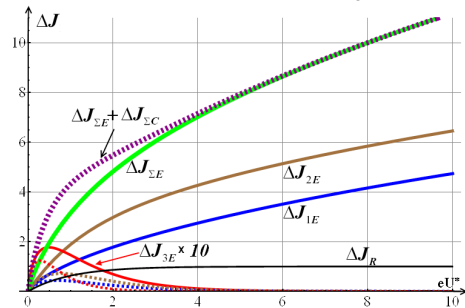


**Figure 4.** Ballistic additives to the Richardson current: emitter - solid colored lines, collector - dotted lines corresponding to the emitter lines of the color, purple dotted line - full addition to the Richardson differential current (to the black line).

As shown in Figure 4, when the potential difference across the barrier is greater than the average thermal energy of electrons ( $eU^* > 1$  false), the first and second ballistic additives significantly exceed the Richardson saturation current. Moreover, the second addition due to electrons with small negative starting velocities, the speed of which changes sign due to the electric field, even exceeds the first addition of accelerated electrons without changing the sign of their velocity. But all these 3 additives, both separately and naturally - total, as will be further shown below, and at low voltages significantly exceed the Richardson difference current, which is fundamentally “immeasurable” at low

voltages (formula 3).

At low voltages, it is necessary to take into account the partial contributions to the anti-accelerated electrons of the collector (dashed lines in Figure 4), which are opposite in sign to the Richardson current of the collector, but similarly exponentially decrease with increasing voltage:

$$J_{R2}^* = J_{R2} + \Delta J_{1C} + \Delta J_{2C} + \Delta J_{3C} = (-J_{R1} + \Delta J_{\Sigma E}) \cdot e^{-eU^*} \quad (12)$$

The ballistic additives obtained in the calculation of the spatial transition, referred to the differential saturation current of Richardson, are shown in Figure 5. For clarity of this conclusion, the total ballistic weighting and the Richardson differential current are shown in a wide range of potential differences on a double logarithmic scale.

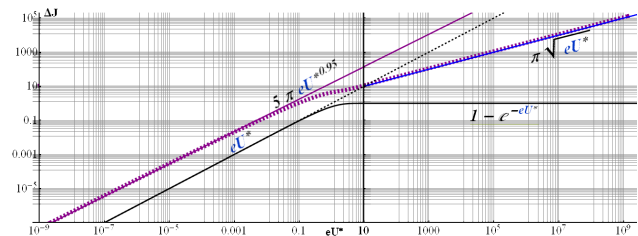


**Figure 5.** Comparison of the total ballistic addition to the barrier current (purple dashed curve) with the Richardson differential current (black curve).

Thus, taking into account the ballistic additions to the Richardson current shows that, on the one hand, the initial portions of the I – V characteristic have significantly large measurable currents, and on the other hand, it shows that the actually observed saturation of the I – V characteristic at high currents (Figure 5, 6) is related to not with the complete depletion of the electronic zone of the emitter, but with the rate at which electrons enter it into its surface layer, i.e. in fact, with resistance, volumetric and surface [18-20].

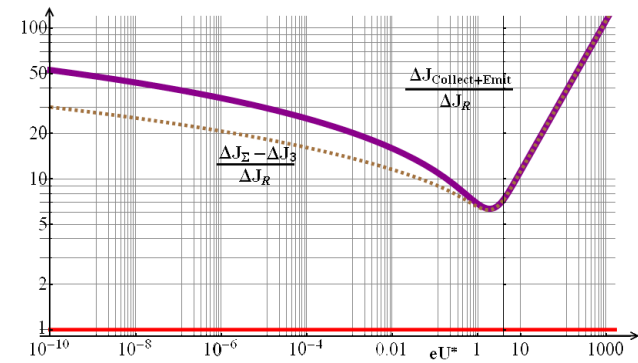


**Figure 6.** The relative increase in the total current due to ballistic effects.

The ratio of the resulting increment of the total current due to ballistic additions to the “immeasurable” at low voltages at the Richardson differential current barrier,

determined only by the concentration force, tends to infinity as the voltage tends to zero:

$$\frac{\Delta J_{\Sigma E} + \Delta J_{\Sigma C}}{\Delta J_R} = \frac{\Delta J_{\Sigma}}{\Delta J_R} \xrightarrow{eU^* \rightarrow 0} \infty \quad (13)$$

We emphasize that the calculation of the current must also take into account those electrons whose velocities are directed away from the barrier, but which, as shown in Figure 3, are able to overcome it according to the law of conservation of energy. This is due to the fact that in the case of chaotic wanderings and collisions of thermal electrons, the laws of conservation of their energy and momentum are also observed. So in momentum space the electrons “swing in the parabolic zones shown in the figures. Therefore, we will consider the spatial transitions of electrons indicated in Figure 2b by green lines.

### 3.2 Generalized Description of Spatial Transitions

The detailed analysis carried out already implicitly took into account the fact that when calculating spatial transitions, it is necessary to take into account the polarity of the kinetic energy (Figure 7). So its record in general:

$$\varepsilon_C^* = \text{Sign}[V_x] \cdot \frac{mV_x^2}{2}$$

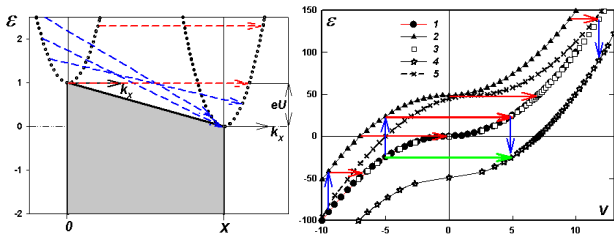


**Figure 7.** Electronic transitions under the action of an electric field when considered in the framework of: standard (left) and taking into account polarity (right) dispersion law.

In Figure 7 on the right: 1 - the initial dispersion law, 2 - the dispersion law, shifted only in energy, 3 - the dispersion law, shifted both in energy and velocity, 4 - a decrease in the potential energy of the obtained dispersion law by an amount equal to an increase in the kinetic energy, 5 - demonstration of displacement of curve 2 by a fixed speed value.

In this case, in contrast to the generally accepted approach [18,19], the record of the total energy is transformed (Figure 7, right):

$$\varepsilon_C^*[x] = \varepsilon_C^*[0] + eEx \rightarrow \text{Sign}[V_x[x]] \cdot \frac{mV_x^2[x]}{2} = \text{Sign}[V_x[0]] \cdot \frac{mV_x^2[0]}{2} + eEx \quad (14)$$

And, as shown in Figure 6 (on the right), expression (14) also gives ballistic transitions with negative initial

velocities, also with conservation of total energy - horizontal lines.

Having solved equation (14) in general form, we obtain an expression for the final velocity of electrons:

$$V_F = \text{Sign}[\text{Sign}[V_S]V_S^2 + A] \sqrt{\text{Abs}[\text{Sign}[V_S]V_S^2 + A]}, \quad \text{где } A = \frac{2eEx}{m} = \frac{2kT}{m} \cdot \frac{eEx}{kT} = b \cdot eU^* \quad (15)$$

In this case, we obtain the final electron velocity  $V_F$  false with a significant addition for small initial electron velocities (Figure 8) and an increase in the flux in the I - V characteristic.

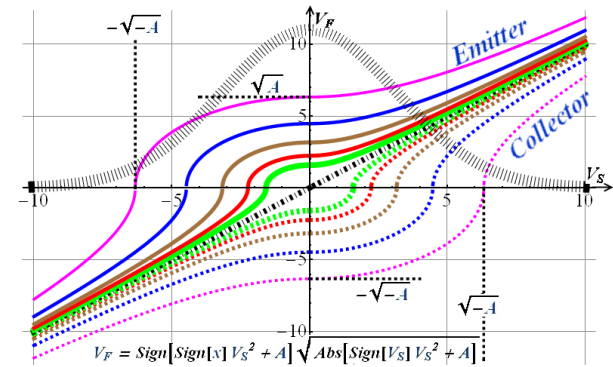


**Figure 8.** Dependences of the final velocity of electrons  $V_F$  false (a) on their initial thermal velocity  $V_S$  false for the emitter and collector. The potential difference changes by a factor of 2 (the broad black dotted line qualitatively shows the distribution of Boltzmann electrons over the initial velocities).

The resulting expression for the final velocities  $V_F$  false (15) gives an analytical zero crossing, both in the initial velocity and in the stress applied to the barrier (Figure 4). It makes it possible to analyze in detail the contributions of electrons with different initial velocities  $V_S$  false to the total electric current.

The plots presented in Figure 8 demonstrate that there is a singularity in the law of addition of velocities near the zero initial velocity of electrons in the parabolic zone. This feature is a consequence of the root dependence of the sum of squares, taking into account the sign of the velocity.

Taking into account the Boltzmann distribution shown by the wide dotted line in Figure 8 for the one-dimensional case, one can obtain [20] the partial contributions of changes in the electron velocities to the total electron flux (Figure 9):

$$dQ^{1D} = e^{-\left(\frac{x^2}{b} + \phi\right)} \left( \left( \text{Sign}[\text{Sign}[x]x^2 + beU^*] \right) \text{Abs} \text{Sign} x x beU x, \sqrt{\left( \text{Abs}[\text{Sign}[x]x^2 + beU^*] \right) - x}, x \equiv V_S \right) \quad (16)$$

Integration of all these partial contributions for the emitter and collector and their summation gives all the ballistic additions obtained above (f. 15 and 16,) as areas under the curves shown in Figure 9.

And, at the same time, as can be seen from Figure 9, the singularity in the change / increments of the final velocity near zero initial velocities is additionally enhanced by the concentration maximum of the Boltzmann distribution.

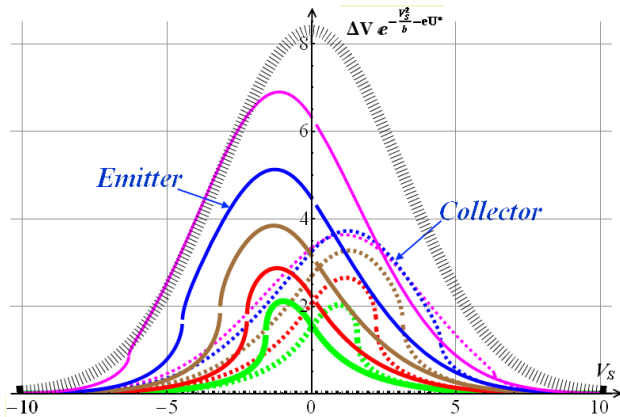


Figure 9. Partial contributions of changes in the initial velocities of the emitter and collector electrons

Integration of partial contributions over the entire range of initial electron velocities brings us back to the formula for the total current (11, 12) with the contributions strictly described by formulas (7-10).

Further refinement of the obtained analytical expressions for the electron fluxes over the barrier requires additional analysis of the shift of the center of gravity of the Boltzmann distribution over the initial electron velocities. A complete simulation of this shift, requiring both the density and free allowed states, will not be carried out in this work, but this qualitatively increases the partial contribution of electrons that were discarded by Richardson from consideration. Will mark only the main thing. The Richardson differential current describing the macroscopic experiments was actually diffuse - an increment due to the field of the average diffuse velocity was used. Whereas the rigorous calculation carried out gives ballistic additions to the current, which are an order of magnitude higher than the diffuse Richardson current. And as can be seen from the above analysis - the maximum additions due to the acceleration of electrons ejected earlier from consideration with negative velocities.

### 3.3 Allowed Spatial Transitions in the p-n Junction

When analyzing and calculating currents above the barrier, it is necessary to take into account not only the electric force,

but also the concentration force arising at the boundary [21]. Without taking it into account, even a rough description of the work of the p-n junction cannot be built.

But, as experiments have confirmed, it is also required to take into account the temperature force that gives the Local Thermal EMF of the barrier. With the traditional Richardson approach to calculating currents, even the Richardson constant could not be used for quantitative estimates and was actually chosen from fitting a small portion of the I – V characteristic, and the I – V characteristic based on the Richardson difference current did not agree well with the experimentally observed one.

For the three-dimensional case, the resulting total fluxes (10, 11) do not change fundamentally - they have only an additional factor, like the three-dimensional Richardson current. In other words, the excess of the three-dimensional ballistic current in relation to the three-dimensional Richardson current remains, which removes the “ban” on the MEASURABILITY of Local Thermal EMF, arising, in particular, in the n-n junction (Figure 10).

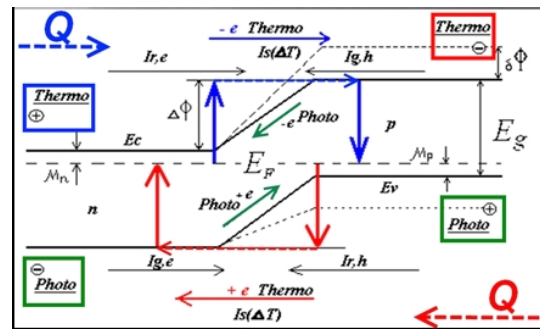


Figure 10. Scheme of the photoelectric effect and the longitudinal thermoelectric effect in the p-n junction

At the same time, as shown in Figure 10, in the n-n junction, along with the photo-EMF (green arrows), the opposite sign, but almost equal in magnitude, Local Thermo-EMF, independent, in contrast to the Seebeck coefficient, of the direction sign heat flow ..

And the values of local thermoelectric currents not only provide MEASURABILITY of “anomalous effects” [22,23], but also give a higher efficiency of energy conversion [24].

Along with the longitudinal, with respect to the heat flux propagating through the n-n junction, the local thermoelectric effect is also observed the so-called transverse local thermoelectric effect [25]. In this case, the appearance of a voltage at the n-n junction during the flow of heat along the boundary of layers with an inverse type of conductivity. This local thermoelectric effect in-phase photoelectric effect gives a significant excess of sensitivity and signal-to-noise ratio in comparison with

standard photodetectors (Figure 11).

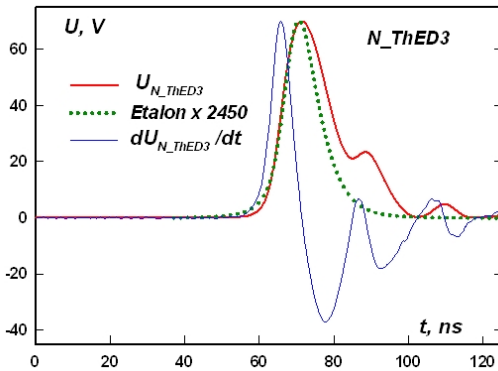


**Figure 11.** Comparison of sensitivity of the thermal receiver (detector) on transversal ( $N_{ThED}$ ) Local Thermo-EMF in p-n junction with the reference photodetector – 10 are used nanosecond impulse of green light.

Thus, both local thermoelectric effects in p-n junction, both longitudinal and transverse, demonstrate not only MEASURABILITY, but their high efficiency.

#### 4. Instead of a Conclusion

Removal of the Richardson-Langmuir Ban made it possible to explain the experimentally observed high signal-to-noise ratio in thermal detectors based on Local Thermo-EMF (Figure 11), which is directly related to their high conversion efficiency (Figure 12).

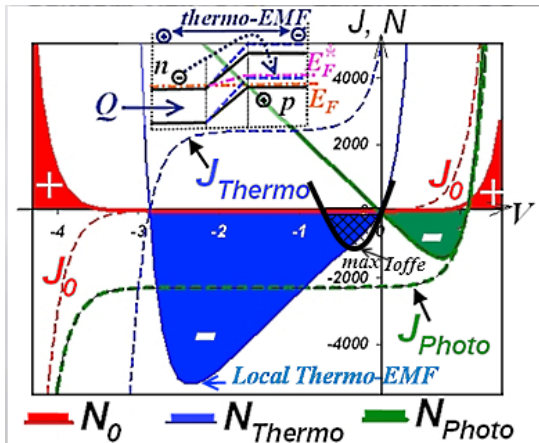


**Figure 12.** Elements imbalance energy in p-n junction: consumption - «+», generation - «-»

As shown in Figure 12, Local Thermo-EMF allows, in principle, to go from the low-voltage maximum Ioffe efficiency for diffuse semiconductors, the theoretical limit of which is less than 16% (practical - less than 12%) to the high-voltage maximum efficiency, which, for local Thermo-EMF, in principle, can exceed 36%.

For generators based on Local Thermo-EMF, the efficiency, like any heat engine, increases with an increase in the operating temperature drop. Therefore, for generators, multilayer structures of nn junctions are required and, preferably, with an increase in the band gap from the radiator to the heater, a number of conjugated nn junctions are needed: Ge-Si-GaAs-GaN<sup>[26]</sup>. In principle, it is possible to use polar superstructures that are stable in the operating temperature range based on incommensurate crystals of higher manganese silicide<sup>[27]</sup>, doped with iron (to reduce their electrical conductivity), or on the basis of silicon carbide polytypes<sup>[28,29]</sup>. But superstructures must be polarized under current and at temperatures below their thermodynamic decomposition, but above the maximum operating temperature of the generator.

#### References

- [1] Ordin S.V., “Non-Elementary Elementary Harmonic Oscillator”, American J Mater Appl Sci (AJMAS). 2021, March 08;3(1): 003-008 p.
- [2] Stanislav V. Ordin, « Impedance of Skin-Plasma Effect», International Journal of Engineering Research and Development (IJERD), , Volume 16, Issue 12, Version - 1 (December 2020),e-ISSN: 2278-067X, p-ISSN: 2278-800X, Ref id AB911011, Impact Factor 4,61.
- [3] Ordin, S.V., «CHAOS – IMAGINARY OSTENSIBILITY – ORTHOGONALITY», Global Journal of Science Frontier Research- Physics & Space Science (GJSFR-A), Volume 19 Issue 3 Version 1.0 p.49-58.
- [4] Ordin S.V., Refinement and Supplement of Phenomenology of Thermoelectricity, American Journal of Modern Physics, Volume 6, Issue 5, September 2017, Page: 96-107.  
DOI: 10.11648/j. ajmp. 20170605. 14.
- [5] S.V. Ordin, “Experimental and Theoretical Expansion of the Phenomenology of Thermoelectricity”, Global Journal of Science Frontier Research- Physics & Space Science (GJSFR-A) Volume 18, Issue 1, p. 1-8, 2018.
- [6] Ordin S.V., “Cardinal increase in the efficiency of energy conversion based on local thermoelectric effects”, International Journal of Advanced Research in Physical Science, Volume-4 Issue-12, p. 5-9, 2017.
- [7] Ordin S.V., Zjuzin A. Yu., Ivanov Yu. and Yamaguchi S., Nano-structured materials for thermoelectric devices, NATO Workshop “Advanced Materials and Technologies for Micro/Nano-Devices, Sensors and Actuators” June 29 - July 2, 2009, St Petersburg, Russia.
- [9] S. V. Ordin, A. J. Zjuzin, Yu. Ivanov, S. Yamaguchi, «Nano-structured materials for thermoelectric devic-

- es», The 29th International Conference on Thermoelectrics, May 30 ~ June 3, 2010 Shanghai, China, P1-14.
- [10] A.M. Filachev, I. I. Taubkin, M.A. Trishenkov, "SOLID STATE PHOTOELECTRONICS (Photodiodes)", Moscow, publishing house "FIZMATKNI-GA"( Physics and Mathematics Book), 2011, 448 pages.
- [11] S.V. Ordin, W.N. Wang, "Thermoelectric Effects on Micro and Nano Level.", *J. Advances in Energy Research*, Volume 9, 2011, p.311-342.
- [12] Thermionic converters and low-temperature plasma, ed. B. Ya. Moyzhes and G.E. Pikusa, M., Nauka, 1973, 532 pp.
- [13] N.A. Arkfen, H. Mermin, *Solid State Physics*, Москва, ИздательствоWorld, 1979, 2 v.
- [14] Jan Tauc, *Photo - and thermo-electric phenomena in semiconductors*, Moscow, Publishing House of the Foreign Literature, 1962, 254 pp.
- [15] S.V. Ordin, «"Anomalies in Thermoelectricity and Reality are Local Thermo-EMFs», *Global Journal of Science Frontier Research- Physics & Space Science (GJSFR-A)*, Volume 18 Issue 2 Version 1.0, p. 59-64, 2018.
- [16] A.F. Ioffe, *Semiconductor thermoelements*, Moscow-Leningrad, Publishing house of the Academy of Sciences of the USSR, 1960, 188 p.
- [17] L.S. Stilbans, *The thermoelectric phenomena, in the book: Semiconductors in a science and engineering*, v. I, Moscow - Leningrad., Publishing house an Academy of Sciences USSR, 1957, p. 113 - 132.
- [18] C.M.Sze, *Physics of Semiconductor Devices*, A Division of John Wiley and Sons, New York, London, 1969, 310 pp.
- [19] V.I. Gamache, *Physics of Semiconductor Devices*, Second Edition, Moscow-Novosibirsk-Tomsk, NTL Publishing House, 2000, 426 pp.
- [20] Stanislav Ordin, *Book: "Refinement of basic physical models"*, Lambert, 2017, ISBN: 978-3-659-86149-9, 82 pp.
- [21] F. Bechstedt, R. Enderlein, *Semiconductor Surfaces and Interfaces*, *Physical Research V.5*, Akademie-Verlag Berlin, 1988, 484 pp.
- [22] J.M. Ziman, *Principles of the theory of solids*, Cambridge, University Press, 1972, 450 p.
- [23] E. H. Roderick, *Metal-semiconductor contacts*, M., Radio and communication, 1982, 231p.
- [24] S.V. Ordin, LOCAL (NANO) THERMOELECTRIC EFFECTS, *Journal of Modern Technology and Engineering (ISSN 2519-4836)*, Vol.5, No.1, 2020, p. 107-109.
- [25] S.V. Ordin et al., "Investigation of the possibility of creating wide-spectrum uncooled sensors for laser radiation identification", abstracts of the scientific and practical conference "Modern Trends and Principles of Optoelectronic Systems Construction" February 9-10, 2012, ROSTEHOLOGY, UOMZ, abstracts p. 62-63, 2012. ISBN: 978-5-85-383-486-6.
- [26] S. V. Ordin, Yu. V. Zhilyaev, V. V. Zelenin, V. N. Panteleev, *Local Thermoelectric Effects in Wide-Gap Semiconductors*, *Semiconductors*, 2017, Vol. 51, No. 7, pp. 883–886. DOI: 10.21883/FTP.2017.07.44643.29.
- [27] S.V. Ordin, *Book: Optical Lattices: Structures, Atoms and Solitons*, "Giant spatial dispersion in the region of plasmon-phonon interaction in one-dimensional- incommensurate crystal the higher silicide of manganese (HSM)", Editors: Benjamin J. Fuentes, Nova Sc. Publ. Inc., 2011, pp. 101-130. 241, ISBN: 978-1-61324-937-6.
- [28] Y. Okamoto, S.V. Ordin, T. Miyakawa, *Journal of Applied Physics*, v.85,9, 1999, p. 6728 -6737, IR-characterization of sintering SiC termoelectric semiconductors with use of 4-component effective medium model.
- [29] Ordin S.V., Sokolov I.A., *Dimension Effect in Lattice Absorption of Silicon Carbide*, *Technical Digest of the 7th International Conference on Optical Technology, Optical Sensors and Measuring techniques 30 May-1 June 2005 Nuremberg Exhibition Centre, Germany, OPTO2005 conference paper 9*, p. 121-124.